

# Experimental investigation of shock waves excited in metals by an intense relativistic electron beam

B. A. Demidov and A. I. Martynov

(Submitted 25 July 1980)  
Zh. Eksp. Teor. Fiz. 80, 738-744 (February 1981)

The spatial attenuation law of intense shock waves excited by pulsed intense relativistic electron beams in duraluminum and copper has been experimentally determined. The results are compared with those experimental and theoretical investigations of hypervelocity impact. It is pointed out that many phenomena produced by hypervelocity impact or explosion near a surface, and in particular, crater formation, can be simulated by means of pulsed intense electron beams.

PACS numbers: 61.80.Fe, 62.50. + p

In connection with the study of hypervelocity meteorite impact, meteorite danger in cosmic flights, the problem of crater formation on the moon and planets, interest has developed in the mechanism of crater formation and the excitation of shock waves by hypervelocity impact and explosion near a surface.<sup>1</sup> Modeling of the many phenomena mentioned above can be carried out with the help of a pulsed intense relativistic electron beam (REB). The technology of contemporary pulsed high-current REB accelerators allows us to obtain in beam self-focusing power densities that exceed  $10^{12}$  W/cm<sup>2</sup> at the focal spot on the anode. The release of energy in a thin anode layer determined by the penetration depth of the electrons in the material of the anode over the time of the pulse ( $\tau \leq 10^{-7}$  s), at the power density described above, leads to a thermal explosion of the anode surface. The vapor of the material, which expands at large velocity, carries a significant momentum.<sup>3</sup> Strong shock waves are thus produced in the investigated material, and in turn produce a crater and structural changes in the material of the anode.<sup>4</sup>

In the present work, the law of spatial damping of shock waves in copper and duraluminum anodes has been determined on the basis of the measurement of the velocity of the shock wave propagating in the anode along the axis of the electron beam. The value of the maximum pressure in the focal spot of the REB has also been calculated. A comparison is presented of the results with theoretical and experimental hypervelocity impact investigations.

## 1. SCHEME OF EXPERIMENT AND EXPERIMENTAL RESULTS

The experiments were carried out on the intense pulsed electron accelerator "Kal'mar"<sup>5</sup> in the following regime: energy of the electrons 350 keV, beam current 110 kA, duration of the beam of relativistic electrons at half-height of the current 50 ns, diameter of the focal spot 1.6 mm, energy released by the REB at the focus 1 kJ.

The experimental setup is shown in Fig. 1. The intense REB 1 is emitted by the cathode 2 and falls on the metallic anode 4. Upon interaction of the REB with the anode, a shock wave 3 is excited and propagates into the interior of the anode. Upon emergence of the

shock wave from the outer side of the anode, the surface of the latter begins to move with twice the bulk velocity of the shock wave and closes up the gap 5 due to the presence of a dielectric liner 7 of thickness 0.08 mm, between the anode 4 and the plate 6. A voltage pulse appears in this case on the resistor  $R_3$ , which is the input resistance of the oscilloscope 12-7. This pulse is the result of the discharge of the capacitor  $C_1$  through the resistor  $R_2$ . An example of the resultant oscillogram is shown in Fig. 25. Two peaks of negative polarity are clearly seen in the oscillogram 2b, the first of which is observed at the beginning of the sweep, and the second after some time  $T$ . The first peak, which is due to electromagnetic interference penetrating into the recording circuit, is of identical shape as the oscillogram of the total current of the accelerator, shown in Fig. 2a. The second peak is connected with the closing of the gap 5 by the shock wave. Upon change in the polarity of the battery that charges the capacitance  $C_1$ , the polarity of the first peak remains unchanged, while that of the second changes. The oscillogram 2b allows us to determine the length of time  $T$  from the instant of excitation of the shock wave, which begins 75 ns after the start of current flow (at this instant of time, the power density of the REB is maximal), to the short circuiting of the gap between the anode and the plate. By varying the thickness of the anode, we obtained the dependence of  $T$  on the anode thickness  $X$  for the duraluminum alloy D16

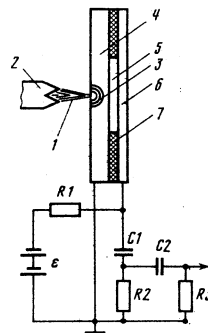


FIG. 1. Experimental setup: 1—REB; 2—cathode; 3—front of shock wave; 4—anode; 5—gap; 6—metallic plate; 7—dielectric liner;  $R_1=100$  k $\Omega$ ,  $R_2=510$   $\Omega$ ,  $R_3=75$   $\Omega$ ;  $C_1=0.01$   $\mu$ F,  $C_2=680$  pF.

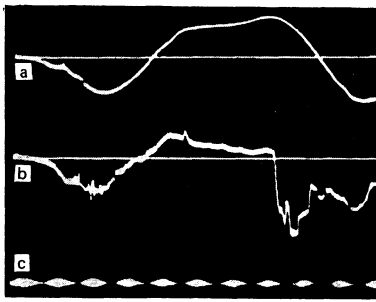


FIG. 2. a) Oscillogram of the total current of the accelerator, b) oscillogram characterizing the velocity of propagation of the shock wave in an anode of copper of thickness 1.5 mm, c) 50 ns, calibration scale.

and for copper mark M1.

The experimental results are shown in Table I, where the averaged values of  $T$ , obtained in several experiments, are given for each thickness of the anode  $X$ .

The experiments were carried out in the same operating regime of the accelerator, and the scatter of the data in the determination of the value of  $T$  for a single thickness of the anode did not exceed 5%. The depth of the hemispherical crater that was formed in thick anodes of duraluminum and copper amounted to 3 mm and 1.5 mm, respectively, in the experiments.

## 2. REDUCTION OF THE EXPERIMENTAL RESULTS

The duration of the time interval  $T_i$  between the instant of excitation of the shock wave and the short circuiting of the air gap between the anode and the plate depends on the anode thickness  $X_i$ , the gap thickness  $\delta$ , and the intensity of the shock wave, and is determined from the following relation

$$T_i = X_i / D_{i,av} + \tau_i, \quad (1)$$

where  $D_{i,av}$  is the average velocity of the shock wave over the length  $X_i$ , and  $\tau_i$  is the time of shorting of the gap, which is approximately equal to  $\delta / 2U_i$  ( $U_i$  is the bulk velocity on the front of the shock at the end of the segment  $X_i$ ).

It is seen from formula (1) that the time of propagation of the shock wave along the anode and the time of shorting of the gap enter into the total time  $T_i$  determined from the oscillogram. The time of shorting of the gap can depend on the voltage applied to the gap, since in the course of action of the shock wave the rear surface of the anode moves, the thickness of the gap decreases in time, and spontaneous breakdown of the gap can take place. With this aim, the voltage applied to the gap was chosen to be an order of magnitude less than that of spontaneous breakdown time, and it was shown in additional experiments that when the bat-

tery voltage  $\varepsilon$  was changed from 30 to 150 V the total time  $\tau_i$  depended only on the intensity of the shock wave in the case of a constant gap and anode thickness. The shock wave velocity  $D$  and the bulk velocity  $U$  are connected by the equation of the shock adiabat:

$$D = a + bU, \quad (2)$$

where  $a$  and  $b$  are constants of the shock adiabat which, according to Ref. 6, are equal respectively to 3.94 km/s and 1.489, for copper and 5.328 km/s, and 1.338 for duraluminum alloy 2024, which is similar in composition to duraluminum mark D16.

Since the bulk velocity, which corresponds to the velocity of the shock wave at the end of the segment  $X_i$ , and not the average bulk velocity  $U_{i,av}$ , enters into formula (1), it is not possible, by using the data of Table I, to solve the set of equations (1) and (2) directly and find the values of the bulk velocity and shock-wave velocity at the various distances  $X$  from the region of excitation of the shock wave that are of interest to us. But, using the method of successive approximations, we can find the average bulk velocity  $U_{i,i+1}$  over the length of the segment  $X_{i+1} - X_i$ , which represents the difference of the anode thicknesses  $X_{i+1}$  and  $X_i$ . In this case, the bulk velocity  $U_{i,i+1}$  will be close to the bulk velocity corresponding to the central point with the coordinate  $X_{i,i+1}$  on the segment  $X_{i+1} - X_i$ . The coordinate of the central point is found from the relation  $X_{i,i+1} = (X_{i+1} + X_i) / 2$  (for the first segment, the coordinate of the central point  $X_{01}$  was reckoned from the inner boundary of the region of absorption of the electron beam in the anode and with account of the depth  $h$  of the absorption of the beam,  $X_{01} = (X_1 - h) / 2 + h$ ).

The bulk velocity  $U_{i,i+1}$  is determined by the formula

$$U_{i,i+1} = (X_{i+1} - X_i) / b \left[ T_{i+1} - T_i - \frac{\delta}{2} \left( \frac{1}{U_{i+1}} - \frac{1}{U_i} \right) \right] - \frac{a}{b}, \quad (3)$$

where  $X_{i+1}$ ,  $X_i$ ,  $T_{i+1}$ ,  $T_i$  are the data of Table I and  $U_{i+1}$  and  $U_i$  are the bulk velocities at the end of the segments  $X_{i+1}$  and  $X_i$ .

As has already been pointed out above, calculation according to formula (3) has been carried out by the method of successive approximations. In the first stage of the calculation of  $U_{i,i+1}$ , the time of closing of the gaps was neglected, i.e., it was assumed that  $U_i = \infty$  and  $U_{i+1} = \infty$ . In each successive stage of the calculation we used the values of  $U_{i+1}$  and  $U_i$  obtained in the preceding stage to plot point by point the relation  $U_{i,i+1} = f(X_{i,i+1})$ .

Thus, the mean values of the bulk velocity on the front of the shock wave were found as functions of the location of the coordinate of the center of the segment on which this velocity was measured. The results of these calculations are given in Table II. The values of the mean bulk velocity correspond to the bulk velocity at the front of the shock wave at points located at a distance  $X$  from the region of excitation of the shock wave. The total error in the determination of the quantity  $U$ , brought about by errors of determination of the quantities  $T$ ,  $X$ , and  $\delta$ , varied from point to point and did not exceed 20% for duraluminum and 30% for copper. The values of the pressures at the shock-wave front at the points

TABLE I.

Anode number, $i$	Duraluminum		Copper		Anode number, $i$	Duraluminum		Copper	
	$X$ , mm	$T$ , nsec	$X$ , mm	$T$ , nsec		$X$ , mm	$T$ , nsec	$X$ , mm	$T$ , nsec
1	0.8	48	1	170	3	2.5	275	2	440
2	1.5	125	1.5	300	4	4	550	-	-

TABLE II.

Duraluminum, $\rho_0=2,785 \text{ g/cm}^3$			Copper, $\rho_0=8,93 \text{ g/cm}^3$		
X, mm	U, km/s	P, Mbar	X, mm	U, km/s	P, Mbar
0.5	7.2	3	0.47	2.3	1.5
1.15	3.5	0.97	1.25	0.8	0.37
2.0	1.6	0.33	1.75	0.5	0.22
3.25	0.75	0.13			

$X$ , which are given in Table II, were found with the help of the well-known relation

$$P = \rho_0(a + bU)U, \quad (4)$$

where  $\rho_0$  is the density of the anode material.

### 3. DISCUSSION OF THE RESULTS

The value given in Table II for the pressure ( $P = 3$  Mbar) in the region of the focal spot of the REB in duraluminum is identical, within the limits of error, with the value of pressure ( $P = 2.4$  Mbar) found from the formula proposed in Ref. 7 for the pressure at the focus of a pulsed high-current REB:

$$P = 0.3(W/S)^{1/2} \rho_0^{1/2}, \quad (5)$$

where  $W$  is the maximum power of the REB and  $S$  is the area of the focal spot of the REB.

It is also necessary to note that the experimentally obtained law of attenuation of the shock wave is very close to the attenuation law for the shock wave investigated in Ref. 8 in the study of impact of an aluminum ball of diameter 4.8 mm, flying with a velocity of 7.3 km/s, on an aluminum target. For convenience in the comparison of the results, we introduce the dimensionless quantities:  $\bar{X} = (X - h)/L$ ,  $\bar{U} = U/U_0$ , where  $h$  is the thickness of the region in which the electron beam is absorbed,  $U_0$  is the maximum value of the bulk velocity at the front of the shock wave (in the case of impact,  $U_0$  is equal to one half the striker velocity),  $L = v_0^{1/3}$  ( $v_0$  is the volume of the striker or the volume of the electron-beam absorption region). Under the conditions of the described experiments, we have for duraluminum  $h = 0.2$  mm,  $L = 0.74$  mm, and  $U_0 = 7.2$  km/s.

The black circles in Fig. 3 represent experimental data for duraluminum, obtained in the present work, while the black squares are the data of Ref. 8. It is seen that the experimental points lie well on the same curve.

The same figure shows also the results of numerical modeling of the damping of a shock wave excited in aluminum by an intense REB with energy in the beam of 1 kJ.<sup>9</sup> The results of calculations on the damping of the shock wave in the case of a hypervelocity impact of aluminum (velocity 20 km/s) on aluminum<sup>10</sup> and iron (velocity 40 km/s) on iron are also shown.<sup>11</sup> All the points lie on the curve which is described by a function of the form

$$\bar{U} = 1 - \exp(-1/\bar{X}^{1.5}). \quad (6)$$

With the help of this expression we can find the maximal values of the bulk velocity in the region near the REB focal spot, and determine the pressure behind the shock front in this zone. Thus, for example, from the data

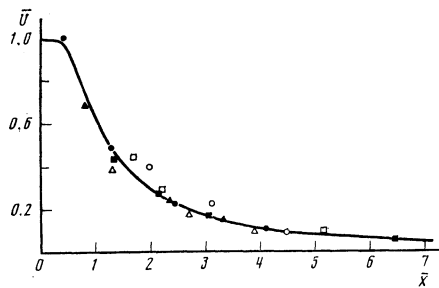


FIG. 3. Dependence of the reduced velocity  $\bar{U}$  on the reduced distance  $\bar{X}$ : ●—described experiment (duralumin anode), ▲—described experiment (copper anode), ■—experiment on the ultra-rapid blow of aluminum on aluminum,<sup>8</sup> △—machine-made experiment on the interaction of the relativistic electron beam with aluminum,<sup>9</sup> ○—calculations on the ultra-rapid blow of aluminum on aluminum,<sup>10</sup> □—calculations on the ultra-rapid blow of iron on iron.

of Table II for a copper anode, using the relation (6), we can easily obtain  $U_0 = 3.07$  km/s, 3.24 km/s, 3.46 km/s, for the first, second, and third points, respectively. Assuming that the mean value of the maximum bulk velocity is 3.27 km/s, we find that the pressure at the REB focal spot is 2.6 Mbar for the copper anode. In Fig. 3, (▲) represents the experimental data for copper, taken from Table II ( $h = 0.06$  mm,  $L = 0.5$  mm). These data also lie satisfactorily close to the continuous curve.

It is necessary to note that at small values of  $X$ , the shape of the striker and the shape of the REB absorption region will also have an effect on the character of the attenuation of the bulk velocity. In finding the values of  $U_0$  from (6) in the case of a highly nonspherical shape of the striker or of the REB absorption region, errors can arise. Evidently, this explains the somewhat lower value of the maximum pressure in experiments with copper ( $P = 2.6$  Mbar) in comparison with the pressure ( $P = 3.5$  Mbar) calculated from formula (5).

The similarity in the character of the attenuation of the shock wave that arises in the interaction of the REB with the anode, and in the hypervelocity impact can be extended to include the determination of the dimensions of the craters obtained in our experiments. An empirical formula is given in Ref. 12 for the determination of the depth of the crater in shock experiments. In the case of a direct impact and a striker and target of the same material this formula takes the form

$$H = 2.28d(V/C_0)^{1/2}, \quad (7)$$

where  $d$  is the diameter of the striker,  $C_0$  is the speed of sound in the target, and  $V$  is the striker speed. This formula can also be used for the determination of the depth of the crater in experiments with intense REB with account taken of the fact that the calculation of the depth in this case must be made with a correction for the thickness of the penetration layer of the electrons in the anode material. With account of this and of the notation adopted, formula (7) takes the form

$$H = 4.5L(U_0/C_0)^{1/2} + h. \quad (8)$$

Calculation according to this formula gives the follow-

ing values for the depth of the craters formed under the action of the intense REB: in duraluminum,  $H = 4.07$  mm, in copper,  $H = 1.97$  mm. This agrees with the experimental results to within 25%.

The good agreement of the experimental results on hypervelocity impact and high-current REB shows that many hypervelocity-impact phenomena can be modeled with the help of a pulsed intense REB. By extrapolating the results, we can hope that upon increase in the energy of the REB to 100 kJ, and at a power density of  $10^{14}$  W/cm<sup>2</sup>, we can model experiments on hypervelocity impact of aluminum on aluminum at speeds up to  $V \approx 50$  km/s.

In conclusion, the authors express their gratitude to S. S. Batsanov and L. I. Rudakov for valued discussions.

<sup>1</sup>In: *Mekhanika obrazovaniya voronok pri udare i vzryve* (Mechanics of Crater Formation in Impact and Explosion), A. Yu. Ishlinskii and G. G. Chennyi, eds. Mechanics series, Mir, Moscow, 1977.

<sup>2</sup>I. P. Afonin, M. V. Babykin, B. V. Baev, *et al.* Papers at the All-Union Conference on Engineering Problems of Thermuclear Reactors, Leningrad, 1977, Vol. II, p. 104, B. A. Demidov, M. V. Ivkin, V. A. Petrov and S. D. Fanchenko,

Atom. energiya 46, 100 (1979).

<sup>3</sup>B. A. Demidov, M. V. Ivkin, V. A. Petrov, V. S. Uglov, and V. D. Chedzhemov, *Zh. Tekhn. Fiz.* 50, 2205 (1980) [Sov. Phys. Tech. Phys. 25, 1285 (1980)].

<sup>4</sup>S. S. Batsanov, B. A. Demidov and L. I. Rudakov, *Pis'ma Zh. Eksp. Teor. Fiz.* 30, 611 (1979) [JETP Lett. 30, 575 (1979)].

<sup>5</sup>B. A. Demidov, M. V. Ivkin and V. A. Petrov, paper at the VI All-Union Conference on Charged Particle Accelerators, Dubna, 1979, Vol. II, p. 67.

<sup>6</sup>R. G. McQueen, S. P. Marsh, J. M. Taylor, J. N. Fritz, and W. J. Carter, *High-velocity Impact Phenomena*, Academic Press, N.Y., 1970.

<sup>7</sup>B. A. Demidov, M. V. Ivkin, V. V. Obukhov, and Yu. F. Tomashchuk, *Zh. Tekhn. Fiz.* 50, 2209 (1980) [Sov. Phys. Tech. Phys. 25, 1288 (1980)].

<sup>8</sup>J. A. Cnarest, General Motors Defense Research Lab. Rept., TR-64-58, 1964.

<sup>9</sup>M. M. Widner and S. L. Thompson, Rept. SLA-74-0272, Sandia Labs, 1974.

<sup>10</sup>J. F. Heyda and T. D. Riney, *Proc. Symp. Hypervelocity Impact*, 7th, 1965, Vol. 3, p. 75.

<sup>11</sup>J. M. Walsh and J. H. Tilletson, *Proc. Symp. Hypervelocity Impact*, 6th, 1963, Part 1, p. 59.

<sup>12</sup>A. C. Charters and J. L. Summers, *Proc. Symp. Hypervelocity Impact*, 3rd, Chicago, 1958.

Translated by R. T. Beyer

## Fluctuation conductivity in $V_3Ge$ near the second critical field

V. A. Marchenko and A. V. Nikulov

*Institute of Solid State Physics, USSR Academy of Sciences*  
(Submitted 25 July 1980)  
*Zh. Eksp. Teor. Fiz.* 80, 745-753 (February 1981)

It is demonstrated by experiment that the superconducting compound  $V_3Ge$  has a fluctuating excess conductivity above the second critical point  $H_{c2}$ . The magnetic-field dependence of the excess conductivity, measured with the field perpendicular to the sample axis, agrees well with the predictions of the theory. The resistivity  $\rho_f$  to the current flow below  $H_{c2}$  is found to deviate from the results of the theory that does not take the fluctuations into account. The agreement of the estimated width of the fluctuation region and of the value of the additional conductivity with the observed region of the anomaly of  $\rho_f$  suggests that the fluctuation mechanism manifests itself also below  $H_{c2}$ .

PACS numbers: 74.40. + k, 74.70.Lp

### INTRODUCTION

It is known<sup>1</sup> that an excess conductivity (paraconductivity) due to fluctuation pairing of the electrons takes place above the superconducting-transition point. In the absence of a magnetic field, i.e., above  $T_c(0)$ , this effect has been sufficiently well investigated, especially in films.<sup>1</sup> In the presence of a magnetic field, the paraconductivity of bulk samples and films has not been sufficiently investigated and the experimental data<sup>2-4</sup> do not agree fully with the theoretical results.<sup>1,5</sup> At the same time, paraconductivity above the second critical field  $H_{c2}$  is of interest because in homogeneous samples the electric resistivity in the  $H_{c2}$  region (disregarding the fluctuations) is finite on both sides of the transition and, according to the prevailing theories,<sup>6</sup> it is close to the resistivity in the normal state

below  $H_{c2}$ . This raises the question of the extent to which the resistivity decreases above  $H_{c2}$  and whether it varies nonmonotonically<sup>7</sup> or monotonically<sup>8</sup> in homogeneous samples on going below  $H_{c2}$ .

Allowance for the fluctuations above  $H_{c2}$  leads in the linear approximation<sup>5</sup> to the following dependence of the excess conductivity  $\Delta\sigma$  on the magnetic field:

$$\Delta\sigma = \frac{\pi}{2\sqrt{2}} \frac{e^2}{h} [\xi(0)]^{-1} F(t, h), \quad (1)$$

where  $\xi(0)$  is the coherence length and  $F(t, h)$  is a universal (independent of the material parameters) function of the relative temperature  $t = T/T_c(0)$  and the relative field  $h = H/H_{c2}$ . Below  $H_{c2}$  the excess conductivity has the same behavior<sup>9</sup> if the current is perpendicular to the field, and differs only by a factor  $\ln[L/\xi(T)]$ ,